Numerical method for analyzing steady-state oscillation in trumpets

Kaburagi, Tokihiko
Faculty of Design, Kyushu University

Kuroki, Chiho
Graduate School of Design, Kyushu University

Hidaka, Shunsuke
Graduate School of Design, Kyushu University

Ishikawa, Satoshi
Faculty of Engineering, Kyushu University

出版情報：Acoustical Science and Technology. 44 (3), pp.269-280, 2023. 日本音響学会
バージョン：

PAPER

Numerical method for analyzing steady-state oscillation in trumpets

Tokihiko Kaburagi[1,*], Chiho Kuroki[2], Shunsuke Hidaka[2] and Satoshi Ishikawa[3]

[1]*Faculty of Design, Kyushu University,*
4–9–1 Shiobaru, Minami-ku, Fukuoka, 815–8540 Japan
[2]*Graduate School of Design, Kyushu University,*
4–9–1 Shiobaru, Minami-ku, Fukuoka, 815–8540 Japan
[3]*Faculty of Engineering, Kyushu University,*
744 Motooka, Nishi-ku, Fukuoka, 819–0395 Japan

(*Received 17 May 2022, Accepted for publication 26 October 2022*)

Abstract: Interactions between the airflow, elastic body of the lips, and acoustic resonator of the instrument cause self-sustained oscillation of the lips when generating sound using brass instruments, and the steady-state oscillation of the instrument can be expected to be periodic. However, quasi-periodic oscillation or period doubling can also occur, and a cascade of period doublings may further introduce chaos. Therefore, given a set of dynamic equations representing the acoustic behaviors of the airflow, lips, and instrument, a method for detecting and obtaining the periodic solution by adopting a shooting method that relies on the match between the initial and terminal states after the time corresponding to the oscillation period has passed is presented in this paper. Experiments were performed for a trumpet model, where the resonance frequency of the lips and the blowing pressure were used as the main control parameters. The minimum blowing pressure was estimated using a linear stability analysis. The method could capture the corresponding changes in the periodic solution very finely when a small perturbation was successively applied to the control parameters; however, it was less effective when the acoustic load of the instrument was capacitive at the oscillation frequency.

Keywords: Trumpet, Two-dimensional lip model, Steady-state oscillation, Shooting method, Linear stability analysis

1. INTRODUCTION

The mechanism of sound generation by brass instruments has been investigated in terms of the resonance characteristics of the instrument bore [1] and the oscillating mechanism of the lips [2–5]. The oscillatory behavior of the lips is influenced by the resonance characteristics of the instrument bore. Therefore, both dynamic systems should be considered simultaneously with the behavior of airflow passing through a narrow channel formed by the upper and lower lips. The vibration of the lips dynamically alters the cross-section of the air channel, which results in a periodic change in the volume flow. Acoustic pressure is generated because of the temporal change in the volume flow, and this is the source of the sound that drives the instrument bore and outputs the instrument sounds. The condition for obtaining the self-sustained oscillation of the reed was theoretically derived by Fletcher [2,3] for pressure-controlled valves. Yoshikawa [4] measured the vibration patterns of horn players and observed the switch between the outward-striking and sideways-striking modes in relation to the blowing pitch. Adachi and Sato presented the results of the computer simulations for the trumpet using a two-dimensional lip model [5].

The steady-state oscillation of the lips can arise when a trumpet is blown with a constant air pressure in the player's mouth, and this can result in periodic changes in the airflow gushing from the air channel and the production of acoustic pressure in the mouthpiece. Periodicity is a key feature of an instrument driven by a self-sustained oscillation mechanism. However, quasi-periodic oscillation (or period doubling) can occur when playing wind instruments, which can create a specific timbre different from that in normal playings. A cascade of period doublings can introduce chaos. Such an instable oscillation of the reed would draw considerable attention and be studied for woodwind instruments [6–9].

However, Gibiat and Castellengo [8] reported empirical data that indicates skilled players of the trombone can intentionally generate quasi-periodic sounds using a special embouchure; this specific performance is different from the

*e-mail: kabu@design.kyushu-u.ac.jp
[doi:10.1250/ast.44.269]

technique that uses vocal folds simultaneously with the lips [10]. Therefore, we can expect that investigations on the occurrence of instable oscillations will help deepen our understanding of the physical mechanisms underlying the performance of brass instruments. Adachi and Sato [5] and Silva *et al.* [11] used computer simulations to show that the oscillating frequency of the lips jumps abruptly when their resonance frequency increases and goes beyond the resonance frequency of the instrument bore. A similar pitch jump phenomenon is observed in the human voice [12–16], and it is referred to as a voice instability. The instability caused when the resonance frequency of the vocal folds increases and goes beyond the resonance frequency of the vocal tract (i.e., the formant frequency) can lead to period doubling and even chaotic behavior of the vocal folds. The existence of hysteresis is a specific feature of a nonlinear system, and it is commonly observed for brass instruments [11] and voice [12] when the resonance frequency of the lips or vocal folds is increased and then decreased.

If the cause of the quasi-periodic oscillations is identified in relation to the values of parameters, such as the lip resonance frequency and blowing pressure, it would help instrument players avoid such undesired blowing states. When the lip behavior is simulated using a set of dynamic equations representing the acoustic behaviors of the airflow, lips, and instrument, the occurrence of quasi-periodic oscillations should be investigated over an extensive range of parameter values. Therefore, the automatic detection of periodic or quasi-periodic oscillation is a crucial but challenging problem. Toward this end, Doc *et al.* [9] employed support vector machine (SVM) to classify periodic and quasi-periodic oscillations. SVM is a machine learning technique; it requires parameter training to construct the boundary between different classes. In general, the effectiveness and classification accuracy decrease for open data in machine learning techniques.

A numerical method called the shooting method [17,18] is adopted in this study to overcome this problem. This method relies on the match between the initial and terminal states, wherein the time interval between both states corresponds to the oscillation period, and the terminal state is derived by numerically integrating the dynamic equations with the given initial state. The problem of finding a periodic solution results in the determination of the value of the initial state. In addition, the oscillation period can be jointly determined based on a nonlinear iterative optimization procedure to minimize the error between the initial and terminal states. Convergence is obtained if the error becomes sufficiently small through iterative optimization, and simultaneously, the existence of a periodic solution is suggested. The method is useful for investigating the occurrence of instability in relation to blowing conditions.

The oscillatory behavior of the lip was represented using a two-dimensional model to examine the effectiveness of the shooting method [5]. In combination with the dynamic models of the airflow and the instrument, the minimum blowing pressure was first estimated with a linear stability analysis to determine the base condition of the control parameters, i.e., the lip resonance frequency and blowing pressure. Then, a small perturbation is successively applied to the parameter values. The primary concern here is the detection of the steady, periodic oscillation; however, we also examine the change in the oscillation period and temporal pattern of the oscillation as a response to the perturbations. We focus on the influence of the resonance characteristic of the instrument bore because it determines the relationship between the volume flow that passes through the lip orifice and acoustic pressure in the mouthpiece. In addition, the relationship between the resonance frequency of the lip and that of the instrument is essential for the occurrence of an abrupt jump in oscillation frequency.

This paper is organized as follows. Section 2 provides a description of the shooting method and the dynamic model representing the acoustic behaviors of the airflow, lip, and instrument. In addition, a method is presented to determine the minimum value of the blowing pressure at which the lip can start the oscillation. In Sect. 3, the numerical results are presented when the values of the control parameters are varied. Finally, Sect. 4 provides a discussion of the experimental results and conclusions drawn from the presented results.

2. ANALYSIS METHOD

The mathematical framework of the analytical method is described in this section. A numerical shooting method is used to obtain the periodic solution of a nonlinear dynamic system. A set of equations representing the mechanical motion of the lip, aerodynamic behavior of the airflow through the lip aperture, and acoustic characteristics of the instrument bore are provided to examine the steady periodic oscillation in the trumpet. Further, we show a linear stability analysis method for determining the minimum blowing pressure with which oscillation of the lip can arise.

2.1. Estimation of the Periodic Solution for a Dynamic System

We assume that the dynamic system representing the performance of the trumpet obeys a set of differential equations.

$$\dot{\boldsymbol{x}}(t) = \boldsymbol{f}(\boldsymbol{x}(t)), \tag{1}$$

where $\boldsymbol{x}(t)$ represents a vector indicating the state of physical variables such as the displacement of the lip, volume flow through the lip aperture, and acoustic pressure in the mouthpiece. The nonlinear function $\boldsymbol{f}$ represents the relationship between these state variables and the input force, i.e., the blowing pressure. When the system is driven, all physical variables change periodically in the steady state such that

$$\boldsymbol{x}(t+T) = \boldsymbol{x}(t), \tag{2}$$

where T represents the oscillation period, and $1/T$ represents the fundamental frequency. If the initial condition $\boldsymbol{x}(0)$ is appropriately given, Eqs. (1) and (2) suggest the relationship

$$\boldsymbol{x}(T) = \int_0^T \boldsymbol{f}(\boldsymbol{x}(t))dt + \boldsymbol{x}(0) \tag{3}$$

and

$$\boldsymbol{x}(T) = \boldsymbol{x}(0). \tag{4}$$

Therefore, the periodic solution of $\boldsymbol{x}(t)$ representing the steady-state oscillation in the trumpet can be obtained by determining the appropriate initial condition, $\boldsymbol{x}(0)$, and the oscillation period, T.

In addition, the variational equation of Eq. (1) is

$$(\dot{\delta\boldsymbol{x}}) = \boldsymbol{J}\delta\boldsymbol{x}, \tag{5}$$

where $\boldsymbol{J}$ is the Jacobian matrix. The (i, j) component of the Jacobian matrix, $\boldsymbol{J}_{ij} = \partial\boldsymbol{f}_i/\partial\boldsymbol{x}_j$, is expressed by the ith component of $\boldsymbol{f}$ and the jth component of $\boldsymbol{x}$. The solution to this initial-value problem can be written as

$$\delta\boldsymbol{x}(t) = \boldsymbol{\Phi}(t)\delta\boldsymbol{x}(0), \tag{6}$$

where $\boldsymbol{\Phi}(t)$ is the state transition matrix. It obeys the relationships

$$\dot{\boldsymbol{\Phi}}(t) = \boldsymbol{J}\boldsymbol{\Phi}(t) \tag{7}$$

and

$$\boldsymbol{\Phi}(0) = \boldsymbol{E}, \tag{8}$$

where $\boldsymbol{E}$ is the unit matrix, and the solution can be written as

$$\boldsymbol{\Phi}(t) = \exp\left(\int_0^t \boldsymbol{J}dt\right). \tag{9}$$

To determine the initial condition, $\boldsymbol{x}(0)$, and the oscillation period, T, we use a numerical scheme (i.e., the shooting method) designed for the solution and stability analysis of steady, periodic vibration problems [17,18]. If $\delta\boldsymbol{x}(t)$ and δT are slight variations in $\boldsymbol{x}(t)$ and T, respectively, the following relationship can be established from Eq. (4):

$$\boldsymbol{x}(T+\delta T) + \delta\boldsymbol{x}(T+\delta T) = \boldsymbol{x}(0) + \delta\boldsymbol{x}(0). \tag{10}$$

When the values of $\boldsymbol{x}(0)$ and T are specified, the values of $\delta\boldsymbol{x}(0)$ and δT can be determined by solving the following simultaneous equations [18]:

$$[\boldsymbol{\Phi}(T) - \boldsymbol{E}]\delta\boldsymbol{x}(0) + \boldsymbol{f}(\boldsymbol{x}(T))\delta T = \boldsymbol{x}(0) - \boldsymbol{x}(T), \tag{11}$$

which can be obtained using linear approximation of Eq. (10) and the relationships in Eqs. (1), (5), and (6). The values of $\boldsymbol{x}(0)$ and T can then be updated by quantities $\delta\boldsymbol{x}(0)$ and δT such that Eq. (10) is satisfied.

To solve Eqs. (1) and (7) simultaneously, we define a vector $z(t)$ of size $N(N+1)$ as

$$z(t) = (\boldsymbol{x}^{\mathsf{T}}(t)\ \phi_1^{\mathsf{T}}(t)\ \phi_2^{\mathsf{T}}(t)\ \cdots\ \phi_N^{\mathsf{T}}(t))^{\mathsf{T}}, \tag{12}$$

where N, $\phi_i(t)$, and T represent the dimension of the state vector $\boldsymbol{x}(t)$, ith column of the state transition matrix, and transposition, respectively. Equations (1), (7), and (8) indicate that $z(t)$ obeys the differential equation

$$\frac{dz(t)}{dt} = \frac{d}{dt}\begin{pmatrix} \boldsymbol{x}(t) \\ \phi_1(t) \\ \phi_2(t) \\ \vdots \\ \phi_N(t) \end{pmatrix} = \begin{pmatrix} \boldsymbol{f}(\boldsymbol{x}(t)) \\ \boldsymbol{J}(\boldsymbol{x}(t))\phi_1(t) \\ \boldsymbol{J}(\boldsymbol{x}(t))\phi_2(t) \\ \vdots \\ \boldsymbol{J}(\boldsymbol{x}(t))\phi_N(t) \end{pmatrix} \tag{13}$$

with the initial condition

$$z(0) = (\boldsymbol{x}^{\mathsf{T}}(0)\ \boldsymbol{e}_1^{\mathsf{T}}\ \boldsymbol{e}_2^{\mathsf{T}}\ \cdots\ \boldsymbol{e}_N^{\mathsf{T}})^{\mathsf{T}}, \tag{14}$$

where $\boldsymbol{e}_i$ denotes the ith column of $\boldsymbol{E}$.

According to [17,18], the iterative algorithm for determining the optimal values of $\boldsymbol{x}(0)$ and T can be stated as

(i) Set the iteration counter as $i = 0$. Let the initial values of $\boldsymbol{x}(0)$ and T be $\boldsymbol{x}_0^0 = \boldsymbol{x}(0)$ and T^0, respectively.

(ii) Set $z(0)$ in Eq. (14) using $\boldsymbol{x}_0^i$ and integrate the differential equation in Eq. (13) for $0 \leq t \leq T^i$. The value of $z(T^i)$, and at the same time, those for $\boldsymbol{x}(T^i)$ and $\boldsymbol{\Phi}(T^i)$, are then obtained.

(iii) The updating quantities, $\delta\boldsymbol{x}_0$ and δT, are determined by solving the simultaneous equations

$$[\boldsymbol{\Phi}(T^i) - \boldsymbol{E}]\delta\boldsymbol{x}_0 + \boldsymbol{f}(\boldsymbol{x}(T^i))\delta T = \boldsymbol{x}_0^i - \boldsymbol{x}(T^i). \tag{15}$$

Here, a specific component of the state vector is exclude in Eq. (15). The value of this component is *a priori* fixed, and it is not updated in the following step; this means that the corresponding component of $\delta\boldsymbol{x}_0$ is set to zero.

(iv) The values of the initial condition and oscillation period are updated as

$$\boldsymbol{x}_0^{i+1} = \boldsymbol{x}_0^i + w \cdot \delta\boldsymbol{x}_0 \tag{16}$$

and

$$T^{i+1} = T^i + w \cdot \delta T, \tag{17}$$

where w represents the updating weight $(0 < w \leq 1)$.

(v) Calculate the difference between the initial and terminal values of the state variables as

$$\delta \boldsymbol{x} = \boldsymbol{x}(T^{i+1}) - \boldsymbol{x}_0^{i+1}, \tag{18}$$

where $\boldsymbol{x}(T^{i+1})$ can be obtained by integrating the equation in Eq. (1). If the norm of $\delta \boldsymbol{x}$ is smaller than the threshold, the convergence is obtained and the iterative process is terminated. The initial condition is given as $\boldsymbol{x}(0) = \boldsymbol{x}_0^{i+1}$, and the oscillation period as $T = T^{i+1}$. Otherwise, the counter is increased as $i = i + 1$, and the process is repeated from the second step.

The shooting method is advantageous for estimating important temporal information, i.e., the oscillation period, in addition to the initial value of the state variables. The capability of this method can be understood as follows: The right-hand side of Eq. (15) represents the difference between the initial and terminal values of the state variables, and this difference can be reduced by changing the initial value and the oscillation period, as respectively expressed in the first and second terms on the left-hand side. If only the second term is considered, it is suggested with Eq. (1) that the updating quantity of the oscillation period is determined such that

$$\dot{\boldsymbol{x}}(T^i) \cdot \delta T = \boldsymbol{x}_0^i - \boldsymbol{x}(T^i). \tag{19}$$

The left side shows the multiplication of the gradient of $\boldsymbol{x}$ at the terminal time instant and the adjusting value of the period. It corresponds to the change in the state variables under the assumption of local linearity; the error on the right-hand side can be reduced by adjusting the period using the updating quantity δT.

2.2. Dynamic Model of the Trumpet

The trumpet model is composed of dynamic equations representing the mechanical behavior of the lip, airflow through the aperture formed by the upper and lower lips, and acoustic resonator of the instrument bore. The equations explicitly describe interactions among physical variables. Behavior of the lips and airflow described in this study is based on the Adachi–Sato model [5]. However, the acoustic pressure in the mouthpiece should be described using a differential equation; the convolution operation between the volume flow and reflection function is no longer valid.

The motion of the lip are modeled using a mass-spring system, and its shape is represented as a parallelogram, according to the literature [5]. The upper and lower lips are supposed to move symmetrically in terms of the x-axis, forming a cuboid channel between them. Using the positional variables x and y and the velocity variables v_x and v_y, the motion of the upper lip in the horizontal and vertical directions can be represented as

$$\dot{x} = v_x, \tag{20}$$

$$\dot{y} = v_y, \tag{21}$$

$$\dot{v_x} = -\frac{1}{m}\left\{\sqrt{\frac{mk}{Q}}v_x + k\Delta x_0 + 2b\Delta p\Delta y_J\right\}, \tag{22}$$

and

$$\dot{v_y} = -\frac{1}{m}\left\{\sqrt{\frac{mk}{Q}}v_y + k\Delta y_0 - 2b\Delta p\Delta x_J - 2bdp_{\mathrm{lip}}\right\}, \tag{23}$$

where $\Delta x_0 = x - x_0$, $\Delta x_J = x - x_J$, $\Delta y_0 = y - y_0$, $\Delta y_J = y - y_J$, and $\Delta p = p_0 - p$; m, k, and Q represent the mass, stiffness, and quality factor, respectively; x_0 and y_0 represent the neutral position of the lip, and x_J and y_J represent the positions of the joint; p_0, p, and p_{lip} represent the static blowing pressure, acoustic pressure in the mouthpiece, and Bernoulli pressure in the channel between the upper and lower lips, respectively; and finally, b and d represent the width of the lip opening and the thickness of the lip, respectively. The dotted mark over the variable indicates the time derivative.

From the equations governing aerodynamic and acoustic quantities (Eqs. (7) and (8) in the literature [5]), the dynamic equation for the acoustic volume flow, U_{a}, can be expressed as

$$\dot{U}_{\mathrm{a}} = \frac{1}{d}\left\{\frac{S_{\mathrm{lip}}\Delta p}{\rho} + U_{\mathrm{a}}^2\left(\frac{1}{S_{\mathrm{cup}}} - \frac{S_{\mathrm{lip}}}{S_{\mathrm{cup}}^2} - \frac{1}{2S_{\mathrm{lip}}}\right)\right\}, \tag{24}$$

where $S_{\mathrm{lip}} = \max(2by, 0)$, S_{cup}, and ρ represent the area of the lip opening, area of the mouthpiece entry, and average air density, respectively.

The acoustic pressure in mouthpiece p is represented using the mode decomposition scheme as

$$p = \sum_{n=1}^{N_p} p_n, \tag{25}$$

where N_p denotes the number of modal components. In addition, each mode component is dynamically represented by [11,19,20] as

$$\dot{p}_n = q_n \tag{26}$$

and

$$\dot{q}_n = -\frac{\omega_n}{Q_n}q_n - \omega_n^2 p_n + \frac{\omega_n Z_n}{Q_n}\dot{U}, \tag{27}$$

where ω_n, Q_n, and Z_n represent the resonance angular frequency, quality factor, and peak magnitude parameter, respectively, for the nth mode. The input to this system is the time derivative of the total volume flow, $U = U_{\mathrm{a}} + U_{\mathrm{lip}}$, which is the sum of the acoustic volume flow, U_{a}, and the volume flow swept by lip motion, U_{lip}. The time derivative of U_{a} is given by Eq. (24), and that of U_{lip} is expressed as follows based on the literature [5].

$$\dot{U}_{\rm lip} = b\{\Delta x_J \dot{v}_y - \Delta y_J \dot{v}_x\}. \quad (28)$$

The mass and stiffness parameters of the lip were set to $m = 1.5/\{(2\pi)^2 f_{\rm lip}\}$ and $k = 1.5 f_{\rm lip}$, respectively, where $f_{\rm lip}$ represents the lip resonance frequency [5]. Besides the lip resonance frequency ($f_{\rm lip}$) and blowing pressure (p_0), the values of the parameters included in Eqs. (22) and (23) were fixed. $f_{\rm lip}$ and p_0 are parameters used to control the behavior of the lip and aeroacoustics variables because the values of the flow components ($U_{\rm a}$ and $U_{\rm lip}$) and mouthpiece pressure (p) can be determined by the behavior of the lip.

From the dynamic model representation presented above, the vector representing the physical state involved in the trumpet performance is expressed as

$$\boldsymbol{x} = (x, y, v_x, v_y, U_{\rm a}, p_1, p_2, \cdots, p_{N_p}, q_1, q_2, \cdots, q_{N_p})^{\rm T}. \quad (29)$$

Further, the total nonlinear dynamic equations, $\dot{\boldsymbol{x}} = \boldsymbol{f}(\boldsymbol{x})$, and the Jacobian matrix, $\boldsymbol{J}_{ij} = \partial \boldsymbol{f}_i / \partial \boldsymbol{x}_j$, can be constructed using Eqs. (20)–(28) to obtain the periodic solution with the shooting method. The number of state variables, and hence, the number of dynamic equations, is $N = 2N_p + 5$. The Bernoulli pressure, $p_{\rm lip}$, in Eq. (23) is not included in the state vector because it can be computed from the flow equation shown in Eq. (8) of the literature [5] and the values of the state variables such that

$$p_{\rm lip} = p - \rho U_{\rm a}^2 \left(\frac{1}{S_{\rm cup} S_{\rm lip}} - \frac{1}{S_{\rm cup}^2} \right). \quad (30)$$

2.3. Estimation of the Minimum Blowing Pressure

Periodic oscillations are analyzed by changing the values of $f_{\rm lip}$ and p_0. We adopted a method called linear stability analysis to determine the minimum value of p_0 required to cause the oscillation [19,20]. Suppose that the lip is initially in a neutral position and a weak blowing pressure is applied. Then, the lip may open slightly to a certain degree and stay again at a balanced position, and air flows through the lip orifice at a constant speed. The constant lip position and volume flow are the equilibrium solutions of the dynamic equations. The solution is denoted by $x_{\rm e}$ and $y_{\rm e}$ for the position of the upper lip and $U_{\rm ae}$ for the volume flow, and the values of other state variables in Eq. (29) are zero.

The equilibrium solution can be determined by substituting these values of the state variables into the dynamic and flow equations and by solving the following simultaneous equations in terms of $x_{\rm e}$, $y_{\rm e}$, and $U_{\rm ae}$.

$$\frac{1}{2} k(x_{\rm e} - x_0) + bP_0(y_{\rm e} - y_J) = 0, \quad (31)$$

$$\frac{1}{2} k(y_{\rm e} - y_0) - bP_0(x_{\rm e} - x_J) - bd\left\{ P_0 - \frac{1}{2}\rho \left(\frac{U_{\rm ae}}{S_{\rm lip}} \right)^2 \right\} = 0, \quad (32)$$

and

$$p_0 - \rho U_{\rm ae}^2 \left(\frac{1}{2S_{\rm lip}^2} - \frac{1}{S_{\rm cup} S_{\rm lip}} + \frac{1}{S_{\rm cup}^2} \right) = 0. \quad (33)$$

In the vicinity of the equilibrium solution, the linearized function $\tilde{\boldsymbol{f}}(\boldsymbol{x})$ can be written as [19,20]

$$\tilde{\boldsymbol{f}}(\boldsymbol{x}) = \boldsymbol{f}(\boldsymbol{x}_{\rm e}) + \boldsymbol{J}(\boldsymbol{x}_{\rm e})(\boldsymbol{x} - \boldsymbol{x}_{\rm e}), \quad (34)$$

where $\boldsymbol{x}_{\rm e}$ denotes the state vector for the equilibrium condition. The eigenvalues of the Jacobian matrix, $\boldsymbol{J}(\boldsymbol{x}_{\rm e})$, provide information about the stability of the equilibrium solution. The equilibrium is instable and the solution starts oscillating if at least one of the eigenvalues has a positive real part. Simultaneously, the imaginary part of the eigenvalue provides information on the angular frequency of oscillation.

3. NUMERICAL RESULTS

3.1. Experimental Conditions

In the numerical study, model parameters were set according to [5] as $S_{\rm cup} = 2.3 \times 10^{-4}\,{\rm m}^2$, $b = 7.0 \times 10^{-3}\,{\rm m}$, $d = 2.0 \times 10^{-3}\,{\rm m}$, $x_J = 0.0\,{\rm m}$, $y_J = 4.0 \times 10^{-3}\,{\rm m}$, $x_0 = 1.0 \times 10^{-3}\,{\rm m}$, and $Q = 3.0$. y_0 was $3.0 \times 10^{-3}\,{\rm m}$, which was slightly greater than that in the original study. The air density is $\rho = 1.2\,{\rm kg/m^3}$.

The number of modes for modelling the instrument bore was 12 ($N_p = 12$). The values of the mode parameters ω_n, Q_n, and Z_n were set in accordance with the literature [11] to approximate the input impedance curve for the open-valve position of a Yamaha YTR1335 trumpet. For the important modes from the 2nd to the 6th, the resonance frequencies ($\omega_n/2\pi$) were 237.16, 353.89, 473.80, 591.29, and 706.70 Hz, respectively. The quality factor (Q_n) ranges from 29.0 to 38.0, and the magnitude (Z_n) ranges from 38.20 to 62.53. Figure 1 shows the input impedance of the instrument, which is computed as

$$Z_{\rm in}(\omega) = \frac{P(\omega)}{U(\omega)} = \sum_{n=1}^{N_p} \frac{Z_n}{1 + jQ_n \left(\dfrac{\omega}{\omega_n} - \dfrac{\omega_n}{\omega} \right)} \quad (35)$$

using the mode decomposition representation presented in Eqs. (25)–(27).

The nondimensionalization of each state variable was performed for numerical stability when applying the shooting method. Position variables were normalized as $\tilde{x} = x/L_{\rm s}$ and $\tilde{y} = y/L_{\rm s}$, where the standard length was set to $L_{\rm s} = \sqrt{bd}$ using the geometrical parameters of the lip. The dimensionless form of the velocity variables is given by $\tilde{v}_x = v_x/(L_{\rm s}/T_{\rm s})$ and $\tilde{v}_y = v_y/(L_{\rm s}/T_{\rm s})$, where $T_{\rm s} = 1/f_{\rm lip}$

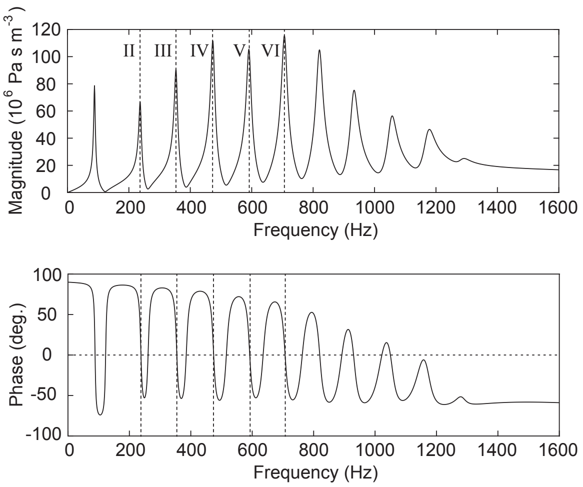

Fig. 1 Magnitude (top) and phase angle (bottom) of input impedance for the instrument bore computed using the mode decomposition representation. The vertical line shows the resonance frequency for each mode from the 2nd to the 6th.

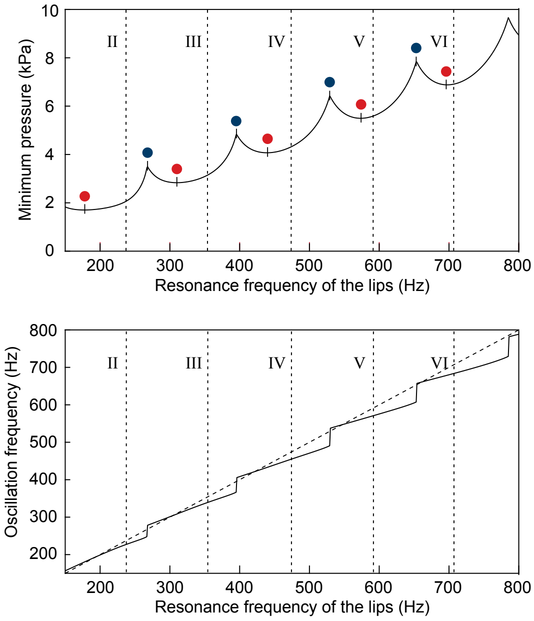

Fig. 2 Estimated minimum blowing pressure (top) and oscillation frequency with the minimum pressure (bottom) as a function of the resonance frequency of the lip. The horizontal line in each graph represents the resonance frequency of the instrument bore corresponding to modes from the 2nd to the 6th. The red circle indicates the frequency at which the minimum blowing pressure was locally minimum, and the blue circle, the frequency at which it was locally maximum.

represents the standard time value. Similarly, the volume velocity was normalized to $\tilde{U} = U/(L_s^3/T_s)$. The standard value of the force is $F_s = mL_s/T_s^2$, by which the dimensionless form of the pressure is given. The dimensionless form of the dynamic equations and Jacobian matrix in Eq. (7) can be obtained by substituting these dimensionless state variables into Eqs. (20)–(28).

In the third step of the shooting method, the value of the state variable representing the y-axis position of the lip was fixed and excluded from the parameter value updating. The updating weight in Eqs. (16) and (17) was changed to $w = 0.1$, 0.5, and 1.0. The optimal value of the weight, and hence, the optimal value of the updating quantity, was determined such that the mean absolute value of the normalized version of the error [$\delta \boldsymbol{x}$ in Eq. (18)] was the smallest. The iterative procedure was terminated when $|\delta \boldsymbol{x}|/N$ was smaller than 2×10^{-4}, or when the number of iterations exceeded hundred as the criterion for convergence. This error criterion was computed for normalized dimensionless variables. The solver function **ode45** of MATLAB (MathWorks Inc.) was used for the numerical integration of dynamic equations.

3.2. Minimum Blowing Pressure

We first investigated the minimum blowing pressure and oscillation frequency with the minimum pressure. In the linear stability analysis, the resonance frequency of the lip (f_{lip}) was changed from 150 to 800 Hz in 1 Hz increments; for each lip resonance frequency, the blowing pressure (p_0) was increased from 1 kPa in 1 Pa increments. The equilibrium solution (x_e, y_e, and U_{ae}), the Jacobian matrix ($\boldsymbol{J}(\boldsymbol{x}_e)$), and its eigenvalues were then computed for each combination of the lip resonance frequency and blowing pressure. The minimum blowing pressure was determined as the pressure at which at least one of the eigenvalues has a positive real part [19,20]. Further, the oscillation frequency was determined as $\omega = \Im(\lambda)$, where $\Im$ represents the imaginary part of a complex number, and λ represents the eigenvalue with a positive real part [19,20].

Top of Fig. 2 shows the estimated minimum blowing pressure as a function of lip resonance frequency. It is evident that the minimum blowing pressure tended to increase with an increase in lip resonance frequency. Further, the curve was U-shaped around each resonance of the instrument, and we observed a pair of local minima and maxima located between the adjacent resonance frequencies of the instrument. These results were in agreements with those performed for a model of the trombone [20]. The lip resonance frequency at each local minimum was below the corresponding resonance frequency of the instrument, and this difference was greater when the mode number was smaller. In general, the lip can oscillate with a small blowing pressure when its resonance frequency is close to the resonance frequency of the instrument.

The bottom plot in Fig. 2 shows the estimated oscillation frequency of the lip driven with the minimum

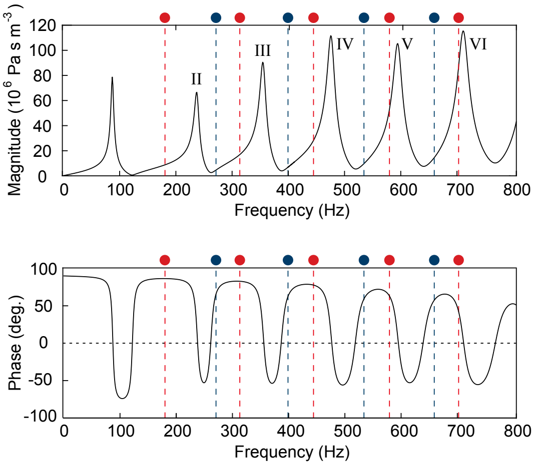

Fig. 3 Magnitude (top) and phase (bottom) of the input impedance of the instrument bore for the frequency range up to 800 Hz. As shown in Fig. 2, the red and blue circles respectively indicate the frequency at which the minimum blowing pressure is locally minimum and maximum.

blowing pressure. The oscillation frequency increased with an increase in lip resonance frequency; however, a discontinuous change in the oscillation frequency was observed between adjacent resonance frequencies of the instrument [5,11]. The minimum blowing pressure increases sharply around the lip resonance frequency when the oscillation frequency leaps, and it forms a steep peak of the minimum pressure. Further, the figure shows that the oscillation frequency was almost lower than the lip resonance frequency, especially around the resonance frequency of the instrument; the oscillation frequency was partially higher than the lip resonance frequency when the leap of the oscillation frequency occurred. This trend was in agreement with the literature [5].

Figure 3 shows the magnitude and phase of the input impedance for the frequency range up to 800 Hz, where the red and blue circles respectively indicate the frequency at which the minimum blowing pressure was locally minimum or maximum, just as in Fig. 2. It is clear from the figure that the phase is positive when the blowing pressure is at the minimum; this suggests that the oscillation of the lip can be initiated effectively for that phase property. However, the frequency marked by the blue circle is slightly above the dip of the input impedance, and in this case, a higher blowing pressure is required to initiate the oscillation of the lip because the acoustic feedback from the instrument is weak.

3.3. Effect of Smooth Change in Blowing Pressure

The oscillatory behavior of the lip was investigated using the shooting method. The blowing pressure was increased from the previously estimated minimum value, whereas the lip resonance frequency was fixed. In the first step of the shooting method, the initial values of the state vector and oscillation period $\boldsymbol{x}_0^0$ and T^0 were given. For the oscillation period, it is reasonable to use the reciprocal of the oscillation frequency estimated by the linear stability analysis (Fig. 2). However, Eqs. (20)–(28) were numerically integrated simultaneously for the duration of $100T^0$, where the stationary state, i.e., the upper lip located at the neutral position and other physical variables were zero, was used as the initial value of the integral. The value of $\boldsymbol{x}_0^0$ was determined by identifying the time instant at which the x-axis value of the lip position was the maximum in the steady state of the oscillation. After normalizing the values of $\boldsymbol{x}_0^0$ and T^0, the shooting method was applied to obtain the optimum solutions of $\boldsymbol{x}(0)$ and T. Then, the blowing pressure was increased with a constant increment, and the solutions $\boldsymbol{x}(0)$ and T were used as $\boldsymbol{x}_0^0$ and T^0, respectively, to analyze the periodic solution for the increased value of the blowing pressure. This procedure was repeated for a certain range of blowing pressures for each condition of the lip resonance frequency.

Figure 4 shows the results for the lip resonance frequency of 220 Hz; the blowing pressure increases from 1,870 Pa, slightly above the minimum value of 1,866 Pa, to 2,300 Pa in increments of 5 Pa. This resonance frequency was used because the phase characteristic of the instrument was close to 90°, as shown in Fig. 3, for which stable oscillation can be expected. The plot in Fig. 4(A) shows the maximum and minimum positions of the lip during the oscillation period. The difference between them (that is, the peak-to-peak amplitude of the vibration) increased continuously with an increase in the blowing pressure. The oscillation frequency plotted in (B) increased almost linearly with an increase in blowing pressure; however, the gradient was very small (approximately 0.004 Hz/Pa). The trajectory of the lip is shown in (C) for blowing pressures of 1,900, 2,000, 2,100, 2,200, and 2,300 Pa. The plots in (D), (E), and (F) show the temporal change in the lip-opening area, total volume velocity ($U_\mathrm{a} + U_\mathrm{lip}$), and mouthpiece pressure (p) for the same blowing pressure values. Plots shown in (C)–(F) were obtained for each blowing pressure by integrating the dynamic equations for the time length of the estimated oscillation period with the estimated initial value of the state vector.

The results demonstrate the effectiveness of the shooting method for obtaining a periodic solution and for examining the effect of blowing pressure on the behavior of the lip and accompanying aeroacoustic variables. Changes in the magnitude and oscillation frequency of the lip motion were reasonably predicted for a gradual increase in blowing pressure. The volume flow increased when the lip opening area increased and the mouthpiece pressure decreased; further, the relationship between the volume

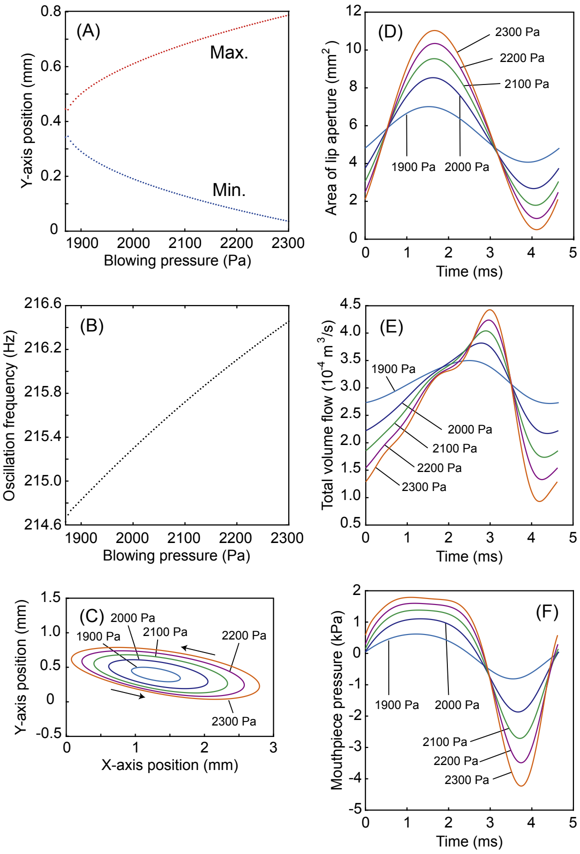

Fig. 4 Estimated results of the steady, periodical oscillation for the lip resonance frequency of 220 Hz. (A) Maximum and minimum positions of the upper lip along the y-axis within the oscillation period. (B) Oscillation frequency. (C) Movement trajectory of the upper lip in the x–y plane for blowing pressures 1,900, 2,000, 2,100, 2,200, and 2,300 Pa. The arrow indicates the direction of elliptical motion. (D–F) Time courses of the cross-sectional area of the lip aperture, total volume velocity, and mouthpiece pressure during the oscillation period. The blowing pressures were 1,900, 2,000, 2,100, 2,200, and 2,300 Pa.

flow and mouthpiece pressure was influenced by the input impedance of the instrument. At an oscillatory frequency of approximately 215 Hz, the phase of the input impedance was positive (see Fig. 3). Therefore, the positive peak of the mouthpiece pressure preceded that of the volume flow over time, as observed in plots (E) and (F). In addition, the positive mouthpiece pressure has an effect of opening the lip and increasing its area, and therefore, the results in (D), (E), and (F) accurately reflect the underlying interrelationships among physical variables. Similar results were obtained for lip resonance frequencies of 178, 310, 440, and 574 Hz, at which the minimum blowing pressure was locally minimum, as shown in Fig. 2.

Figure 5 shows the oscillation frequency of the lip when the blowing pressure was first increased from 1,870 to 2,000 Pa, and then decreased again to 1,870 Pa. A weak

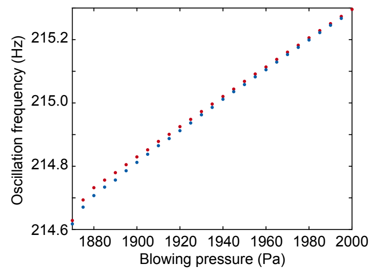

Fig. 5 Oscillation frequency of the lip for when the blowing pressure was first increased (red circle) and then decreased (blue circle). The lip resonance frequency was 220 Hz.

hysteresis was observed, and the difference in the oscillation frequency between the ascending and descending conditions was 0.025 Hz at 1,880 Pa. Hysteresis existed for the lip resonance frequencies of 230, 235, 340, and 450 Hz, where the oscillation frequency was always higher in the ascending condition than in the descending condition.

3.4. Effect of a Smooth Change in the Lip Resonance Frequency

The oscillatory behavior of the lip was examined when its resonance frequency was changed from 180 to 250 Hz in 2 Hz increments. The blowing pressure was 100 Pa greater than the minimum value for each lip resonance frequency, as shown in Fig. 6(A). To apply the shooting method, the initial value of the oscillation period was determined using a linear stability analysis for a lip resonance frequency of 180 Hz. The initial value of the state vector was determined by integrating the dynamic equations starting from the stationary state. When the optimal values of the initial value and oscillation period were obtained, these values were used as the initial values of the optimization after the lip resonance frequency was increased; the procedure was repeated for each condition on the lip resonance frequency.

The oscillation frequency plotted in (C) increased almost linearly as a function of the lip resonance frequency. The two frequencies were almost equivalent when the resonance frequency was 196 Hz; the oscillation frequency was higher than the resonance frequency below this frequency and vice versa. The phase angle of the input impedance plotted in (D) decreased sharply with an increase in the lip resonance frequency above 220 Hz; however, it remained positive.

Based on the results plotted in (B), (E), and (F), the magnitude of lip motion and opening area decreased with an increase in the lip resonance frequency. The peak value of the mouthpiece pressure plotted in (H) did not change significantly irrespective of the lip resonance frequency, although the blowing pressure increased with an increase in

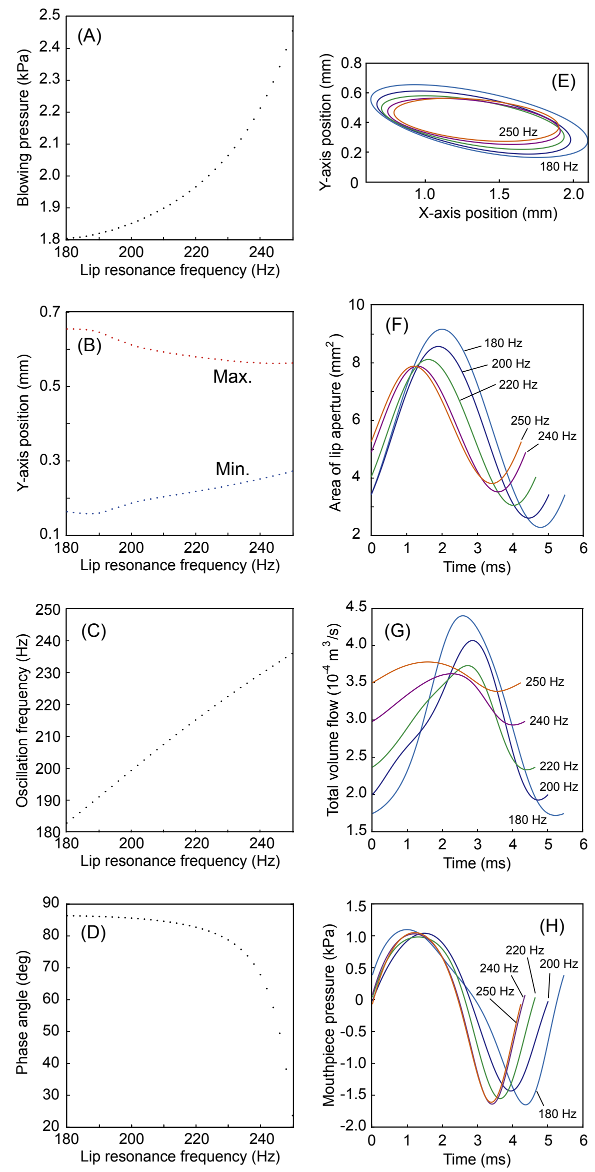

Fig. 6 Estimated results of steady, periodical oscillations when the lip resonance frequency increased from 180 to 250 Hz. (A) Blowing pressure set for each lip resonance frequency. (B) Maximum and minimum position of the lip along the *y*-axis within the oscillation period. (C) Oscillation frequency. (D) Phase angle of the input impedance determined from the oscillation frequency for each lip resonance frequency. (E) Movement trajectory of the lip in the *x*–*y* plane for the lip resonance frequencies of 180, 200, 220, 240, and 250 Hz. (F–H) Time courses of the cross-sectional area of the lip aperture, total volume velocity, and mouthpiece pressure during the oscillation period for lip resonance frequencies of 180, 200, 220, 240, and 250 Hz.

the lip resonance frequency, as shown in (A). The stiffness of the lip increased in proportion to its resonance frequency, which could result in a reduction in the lip opening area. Indeed, the waveforms of the total volume flow plotted in (G) changed significantly depending on the lip resonance frequency. This can be understood from the phase angle of the input impedance plotted in (D), i.e., the peak of the volume flow and that of the mouthpiece pressure coincided with an increase in the lip resonance frequency and a decrease in the phase angle.

The results shown in Fig. 6 clearly demonstrate how the phase angle of the input impedance influences the generation of volume flow. The mouthpiece pressure peaked when the lip-opening area peaked for a lip resonance frequency of 250 Hz. This temporal relationship is not favorable because the positive mouthpiece pressure decreases the pressure difference between the inlet and outlet of the lip opening and prevents the flow generation, whereas the peak of the lip area promotes it. These two factors are therefore contradictory and less effective. In contrast, the temporal relationship was favorable when the lip resonance frequency was 180 Hz: the phase angle was approximately 86°, and the mouthpiece pressure peaked at approximately 1 ms; therefore, this made the pressure difference greater when the lip area opened maximally at approximately 2 ms. As a result, volume flow was generated effectively from a lower blowing pressure.

The oscillation frequency was lower than the lip resonance frequency when it was above 196 Hz. This enlargement of the oscillation period can be explained as follows: the peak location of the mouthpiece pressure was temporally very close to that of the lip-opening area when the lip resonance frequency was 240 or 250 Hz. The peak of the lip area indicates that the upper lip opened maximally at that moment. In addition, the positive mouthpiece pressure gives rise to the upward driving force to the lip. Therefore, this temporal relationship can prevent the lip from closing, which can result in an increase in oscillation period.

3.5. Analysis of the Mode Transition Region

Finally, the existence of a periodic solution was examined for the transition region between the 2nd and 3rd modes of the instrument by altering the lip resonance frequency from 244 to 280 Hz in 2 Hz increments. We found that the blowing pressure needed to be sufficiently greater than the minimum value to obtain a stable periodic solution when the lip resonance frequency was fixed within this range. Thus, the blowing pressure was increased from the minimum value in 10 Pa increments. For each blowing pressure, the initial value of the state vector was determined by integrating the dynamic equations starting from the stationary state, and then, the shooting method was applied.

Figure 7 shows the oscillation frequency as a function of the blowing pressure for each condition of the lip resonance frequency. In the bottom plot, the lip resonance frequency ranges from 244 to 264 Hz. The blowing

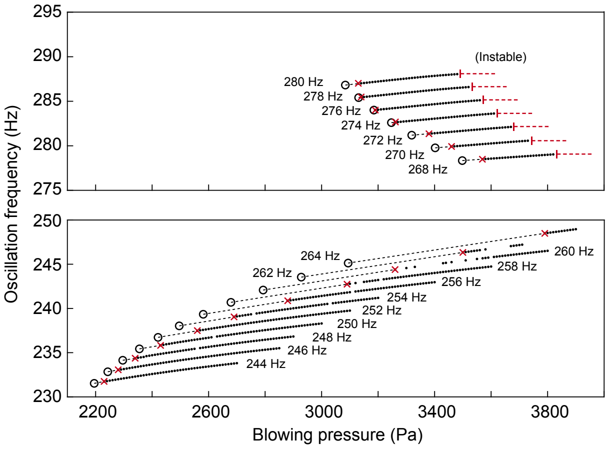

Fig. 7 Estimated oscillation frequency (dot mark) for the lip resonance frequency of 244–256 Hz (bottom) and 268–280 Hz (top). The open circle indicates the oscillation frequency with the minimum blowing pressure; the red cross mark indicates the oscillation frequency with the lowest blowing pressure, by which the periodic solution was obtained with the shooting method. Both marks are connected with the broken line.

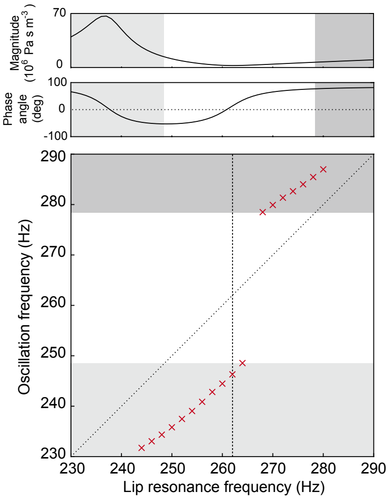

Fig. 8 Oscillation frequency as a function of the lip resonance frequency (red cross mark). The blowing pressure was set to the lowest value by which the periodic solution was obtained. The magnitude and phase angle of the input impedance of the instrument are also illustrated. The gray region in each graph represents the range of the oscillation frequency (below 248.5 Hz and above 278.5 Hz).

pressure is higher than the minimum value determined by linear stability analysis when the lip resonance frequency is higher. In the top plot, the lip resonance frequency ranged from 268 to 280 Hz. The blowing pressure had an upper limit for these resonance frequencies, and the behavior of the lip was instable when the blowing pressure was higher than the limit. Further, we could not find any periodic solutions for the lip resonance frequency of 266 Hz.

The oscillation frequency is shown in Fig. 8 as a function of the resonance frequency of the lip. The blowing pressure was the lowest value with which the periodic solution was obtained using the shooting method, as indicated by the red cross mark in Fig. 7. The dotted vertical line indicates the frequency (262 Hz) at which the magnitude of the input impedance was the minimum between the 2nd and 3rd peaks. The oscillation frequency was lower than the lip resonance frequency when the resonance frequency was lower than or equal to 264 Hz, and vise versa, when the resonance frequency was higher than or equal to 268 Hz. The results imply that the sounding frequency of the instrument could jump [5,11] from the note corresponding to the 2nd mode of the instrument to the note corresponding to the 3rd mode when the lip resonance frequency increased across the local minimum of the input impedance.

Temporal patterns of the *y*-axis position of the lip, total volume flow, and mouthpiece pressure are computed by integrating the dynamic equations to examine the instable behavior of the lip, as shown in Fig. 7. Figure 9 shows the results when the lip resonance frequencies are 274 and

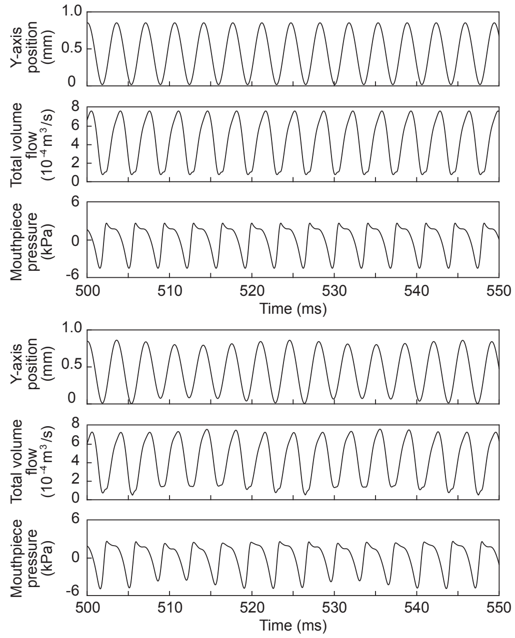

Fig. 9 Simulated temporal patterns of the *y*-axis position of the lip, total volume flow, and mouthpiece pressure for the lip resonance frequency of 274 Hz (top) and 276 Hz (bottom). The blowing pressure was 3,600 Pa.

276 Hz and the blowing pressure is 3,600 Pa. Although the difference in lip resonance frequency was only 2 Hz, the simulated temporal pattern fluctuated from cycle to cycle when the lip resonance frequency was 276 Hz. No convergence was obtained in the iterative procedure of the

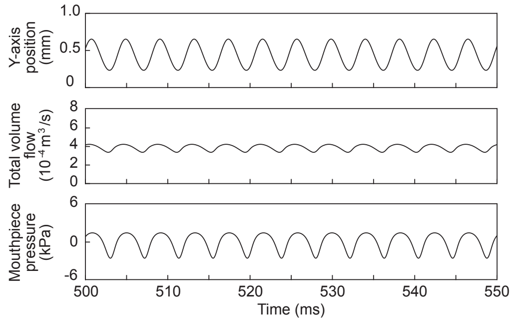

Fig. 10 Simulated temporal patterns of the *y*-axis position of the lip, total volume flow, and mouthpiece pressure for the lip resonance frequency of 256 Hz. The blowing pressure was 2,800 Pa.

shooting method under the condition of the lip resonance frequency and blowing pressure; therefore, a time-domain simulation was required to ensure the existence of instable behavior.

The bottom plot in Fig. 7 indicated a limit for the shooting method. For example, when the lip resonance frequency was 256 Hz, a blowing pressure of 2,880 Pa was required to obtain the periodic solution. However, as illustrated in Fig. 10, a periodic pattern is obtained with the time-domain simulation even when the blowing pressure is lower than 2,880 Pa. In Fig. 8, the oscillation frequency ranges from 237.5 to 248.5 Hz when the lip resonance frequency ranged from 252 to 264 Hz. Within this frequency range, the figure shows that the phase angle of the input impedance is negative. The experimental results imply that the effectiveness of the shooting method depends on the input impedance of the instrument at the oscillation frequency.

4. SUMMARY AND CONCLUSION

A numerical method is presented to estimate the periodic solution of a dynamic system that represents the sound generation mechanism of the trumpet. This method was based on the shooting method [17,18] in which the periodic solution was determined using an iterative procedure by optimizing the initial values of the state variables and oscillation period. Further, linear stability analysis [19,20] was used to estimate the minimum blowing pressure and oscillation frequency at that pressure. The self-sustained oscillation of the lip was represented using a two-dimensional model [5]; the acoustic characteristics of the instrument bore were represented by combining a mode decomposition scheme and dynamic equation considering the volume flow input to the mouthpiece and the resulting acoustic pressure [11,19,20].

Numerical experiments were performed by smoothly changing the resonance frequency of the lip or blowing pressure, or by changing both parameters simultaneously. The results indicated that the shooting method could properly solve the initial value problem. The estimated oscillation frequency of the lip varied finely with a small change in the control parameters. We ensured that the method could be used for both the detection and estimation of the periodic solution, even when the system had a large number of state variables and dynamic equations. Further, the obtained oscillatory behaviors of the state variables were interpretable in terms of the relationship between their temporal waveforms and the input impedance of the instrument at the oscillation frequency.

In the analysis of the transition region between the successive modes of the instrument, the convergence of the solution was not obtained by the shooting method when the lip resonance frequency was around the frequency at which the magnitude of the input impedance was in the locally minima. A jump in the oscillating frequency was reported [5,11] around this specific frequency. Irregular situations in our study were classified into two cases: (1) We confirmed that the behavior of the state variables was no longer periodic when the lip resonance frequency was higher than the frequency of the impedance minimum and the phase of the input impedance was positive. (2) In the other case, the shooting method could not detect the periodic solution when the phase of the input impedance was negative at the oscillation frequency. The former case showed the usefulness of the shooting method for detecting the existence of the instable behavior of the system; however, the latter case exhibited its limitation.

Considering this limitation, we plan to extend the present study to explore the occurrence of the period-doubling phenomenon [8] in the trumpet. The shooting method is directly applicable to the detection of this phenomenon by setting the initial value of the oscillation period in two ways. The optimization procedure of the shooting method does not converge because of fluctuations given by period-doubling when the phenomenon is caused by a small change in the values of the control parameters and the oscillation period is initially set to the regular, periodic solution of the previous parameter setting. Further, if the initial value of the oscillation period is doubled, the optimization procedure works and provides a solution; and therefore, it is possible to detect this phenomenon.

We would like to focus on the acoustic role of the player's vocal tract because we have already revealed how the players of the brass and woodwind instruments control the vocal tract in selecting a specific mode of the instrument and the blowing pitch [21,22]. Acoustic characteristics of the vocal tract can be computed using morphological data obtained using a magnetic resonance imaging device and modeled using a dynamic system representation. Therefore, the effects of the vocal tract can be incorporated into the trumpet model. Future studies can determine the cause of the period-doubling phenomenon and help trumpet players avoid such unwilling blowing states.

REFERENCES

[1] J. Backus, "Input impedance curves for the brass instruments," *J. Acoust. Soc. Am.*, **60**, 470–480 (1976).
[2] N. H. Fletcher, "Excitation in woodwind and brass instruments," *Acustica*, **43**, 63–72 (1979).
[3] N. H. Fletcher, "Autonomous vibration of simple pressure-controlled valves in gas flows," *J. Acoust. Soc. Am.*, **93**, 2172–2180 (1993).
[4] S. Yoshikawa, "Acoustical behavior of brass player's lips," *J. Acoust. Soc. Am.*, **97**, 1929–1939 (1995).
[5] S. Adachi and M. Sato, "Trumpet sound simulation using a two-dimensional lip vibration model," *J. Acoust. Soc. Am.*, **99**, 1200–1209 (1996).
[6] C. Maganza, F. Laloë and R. Caussé, "Bifurcations, period-doublings and chaos in clarinet-like systems," *Europhys. Lett.*, **1**, 295–302 (1986).
[7] T. Idogawa, T. Kobata, K. Komuro and M. Iwaki, "Nonlinear vibrations in the air column of a clarinet artificially blown," *J. Acoust. Soc. Am.*, **93**, 540–551 (1993).
[8] V. Gibiat and M. Castellengo, "Period doubling occurences in wind instruments musical performance," *Acta Acust. united Ac.*, **86**, 746–754 (2000).
[9] J.-B. Doc, C. Vergez and S. Missoum, "A minimal model of a single-reed instrument producing quasi-periodic sounds," *Acta Acust. united Ac.*, **100** (2014). DOI:10.3813/AAA.918734.
[10] L. Velut, C. Vergez and J. Gilbert, "Measurements and time-domain simulations of multiphonics in the trombone," *J. Acoust. Soc. Am.*, **140**, 2876–2887 (2016).
[11] F. Silva, C. Vergez, P. Guillemain, J. Kergomard and V. Debut, "MoReeSC: A framework for the simulation and analysis of sound production in reed and brass instruments," *Acta Acust. united Ac.*, **100**, 126–138 (2014).
[12] J. G. Švec, H. K. Schutte and D. G. Miller, "On pitch jumps between modal and falsetto registers in voice: Data from living and excised human larynges," *J. Acoust. Soc. Am.*, **106**, 1523–1531 (1999).
[13] D. G. Miller, J. G. Švec and H. K. Schutte, "Measurement of characteristic leap interval between modal and falsetto registers," *J. Voice*, **16**, 8–19 (2002).
[14] I. R. Titze, "Nonlinear source-filter coupling in phonation: Theory," *J. Acoust. Soc. Am.*, **123**, 2733–2749 (2008).
[15] Y. Uezu and T. Kaburagi, "A measurement study on voice instabilities during modal-falsetto register transition," *Acoust. Sci. & Tech.*, **37**, 267–276 (2016).
[16] T. Kaburagi, M. Ando and Y. Uezu, "Source-filter interaction in phonation: A study using vocal-tract data of a soprano singer," *Acoust. Sci. & Tech.*, **40**, 313–324 (2019).
[17] T. J. Aprille, Jr. and T. N. Trick, "A computer algorithm to determine the steady-state response of nonlinear oscillators," *IEEE Trans. Circuit Theory*, **CT-19**, 354–360 (1972).
[18] H. Tamura and K. Matsuzaki, "Numerical scheme and program for the solution and its stability analysis for a steady periodic vibration problem," *Trans. Jpn. Soc. Mech. Eng.*, **60**, 30–37 (1994) (in Japanese).
[19] J. S. Cullen, J. Gilbert and D. M. Campbell, "Brass instruments: Linear stability analysis and experiments with an artificial mouth," *Acta Acust. united Ac.*, **86**, 704–724 (2000).
[20] L. Velut, C. Vergez, J. Gilbert and M. Djahanbani, "How well can linear stability analysis predict the behavior of an outward valve brass instrument model?," *Acta Acust. united Ac.*, **103**, 132–148 (2017).
[21] T. Kaburagi, N. Yamada, S. Fukui and E. Minamiya, "A methodological and preliminary study on the acoustic effect of a trumpet player's vocal tract," *J. Acoust. Soc. Am.*, **130**, 536–545 (2011).
[22] T. Kaburagi, A. Kato, Y. Fukuda and F. Taguchi, "Control of the vocal tract when experienced saxophonists perform normal notes and overtones," *Acoust. Sci. & Tech.*, **42**, 83–92 (2021).